Title

Patient-specific finite element modeling of the Cardiokinetix Parachute® device: effects on left ventricular wall stress and function

Authors

Lee, Lik Chuan
Ge, Liang
Zhang, Zhihong
et al.

Patient-specific finite element modeling of the Cardiokinetix Parachute® device: Effects on left ventricular wall stress and function

Lik Chuan Lee, PhD[1,2,4], **Liang Ge, PhD**[1,2,4], **Zhihong Zhang, MS**[4], **Matthew Pease**[5], **Serjan D. Nikolic, PhD**[5], **Rakesh Mishra, MD**[3,4], **Mark B. Ratcliffe, MD**[1,2,4], and **Julius M. Guccione, PhD**[1,2,4]

[1]Department of Surgery, University of California, San Francisco, California

[2]Department of Bioengineering, University of California, San Francisco, California

[3]Department of Medicine, University of California, San Francisco, California

[4]Veterans Affairs Medical Center, San Francisco, California

[5]Cardiokinetix, Inc., Menlo Park, California

Abstract

The Parachute® (Cardiokinetix, Inc., Menlo Park, California) is a catheter-based device intended to reverse left ventricular (LV) remodeling after antero-apical myocardial infarction. When deployed, the device partitions the LV into upper and lower chambers. To simulate its mechanical effects, we created a finite element LV model based on computed tomography (CT) images from a patient before and 6 months after Parachute® implantation. Acute mechanical effects were determined by *in-silico* device implantation (VIRTUAL-Parachute). Chronic effects of the device were determined by adjusting the diastolic and systolic material parameters to better match the 6-month post-implantation CT data and LV pressure data at end-diastole (ED) (POST-OP). Regional myofiber stress and pump function were calculated in each case. The principal finding is that VIRTUAL-Parachute was associated with a 61.2% reduction in the lower chamber myofiber stress at ED. The POST-OP model was associated with a decrease in LV diastolic stiffness, and a larger reduction in myofiber stress at the upper (27.1%) and lower chamber (78.4%) at ED. Myofiber stress at end-systole and stroke volume were little changed in the POST-OP case. These results suggest that the primary mechanism of Parachute® is a reduction in ED myofiber stress, which may reverse eccentric post-infarct LV hypertrophy.

Keywords

Myocardial Infarction; Remodeling; Finite element method; Surgical ventricular restoration

Corresponding Author: Mark B. Ratcliffe, MD, Division of Surgical Services (112), San Francisco Veterans Affairs Medical Center, 4150 Clement Street, San Francisco, California 94121. Telephone: (415) 221-4810. FAX: (415) 750-2181. Mark.Ratcliffe@va.gov.

1. Introduction

The increase in left ventricular (LV) volume that occurs after myocardial infarction (MI) is increasingly recognized as a potential target for therapeutic intervention. In general, this LV remodeling process is thought to be driven by an increase in stress in the LV wall. Specifically, a compensatory increase in end-diastolic volume (EDV) is associated with an increase in end-diastolic stress which causes eccentric hypertrophy of myocardium [1]. Increased end-systolic stress in the MI border zone (BZ) may also lead to non-ischemic infarct extension and subsequent LV enlargement [10].

The Parachute® (Cardiokinetix Inc, Menlo Park, CA) is a catheter-based device intended to reverse LV remodeling after antero-apical MI. When deployed, the Parachute® device partitions the LV into upper and lower chambers. The Parachute® has been shown to reduce LV EDV and end-systolic volume (ESV) in animals [14] and humans [15]. The initial multi-center, phase 1 "Percutaneous Ventricular Restoration in Chronic Heart Failure" or PARACHUTE trial found an improvement in the LV ejection fraction, the New York Heart Association (NYHA) class and the 6-minute walk test [15]. However, it is unclear as to what mechanisms are responsible for these improvements.

Finite element (FE) modeling of the heart and cardiac surgical procedures is becoming more common [4, 21]. Specifically, FE modeling allows the estimation of LV myofiber stress, which is impossible to measure *in vivo* [9]. In addition, the FE method allows inverse calculation of the myocardial material parameters by either manually or automatically adjusting these parameters to match the *in vivo* measured LV strain and volume at different phases of a cardiac cycle [19, 23].

Here, we describe the first patient-specific model capable of simulating the direct interaction between the Parachute® and the LV. This model was reconstructed based on computed tomography (CT) images taken from a patient before and after the device was implanted. The entire implantation process and the effects of Parachute® on LV function and regional mechanics were simulated using contact modeling and a validated user-defined material law for diastolic and end-systolic myocardial mechanics. The goal of this paper is twofold: first, to describe our methodology for simulating such patient-specific effects of the Parachute®; and second, to present preliminary results from this single-patient study.

2. Methods

2.1 Imaging

Imaging was performed using a 64-slice CT scanner (Siemens Medical, Malvern, PA). Image slices were 0.75mm in width with 0.4mm overlap. The image sequence was gated to the surface electrocardiogram and there were 10 R wave to R wave phases. A series of long and short-axis images of the LV were reconstructed and analyzed (Figure 1), and are shown in the animation (Online Resource 1). Computed tomography data acquisition was triggered by the QRS complex of the electrocardiogram.

2.2 Image Analysis

A customized program (iContours, Liang Ge, Cardiac Biomechanics Lab, San Francisco, CA) based on the medical image processing environment Mevislab (v 2.1, Mevislab, Bremen, DE) was used to contour the endocardial and epicardial surfaces of the LV (Figure 2A). Computed tomography images corresponding to end-of-diastole (ED) and end-of-systole (ES) were defined as images where the LV had the largest and smallest cross sectional area, respectively.

2.3 Finite Element modeling

2.3.1 Overview—Finite element models of the LV and Parachute® were created based on the pre-operative (PRE-OP) CT images at early-diastole and the device specifications provided by Cardiokinetix, respectively. To determine acute effects associated with the Parachute® treatment, Parachute® implantation was first simulated on the PRE-OP LV model before simulating ED and ES on the LV model implanted with the device (VIRTUAL-Parachute case). In the post-operative (POST-OP) case, the measured LV end-diastolic pressure (EDP) at 6-months was applied to the LV, and the diastolic and systolic material parameters of the LV were adjusted so that the predicted LV volume agreed with that measured from the 6-month POST-OP CT images. The LV pump function and the myofiber stress at ED and ES were calculated in these 3 cases (PRE-OP, VIRTUAL-Parachute and POST-OP). All the simulations were performed using LS-DYNA (Livermore Software Technology Corporation, Livermore, CA).

2.3.2 PRE-OP finite element model of the left ventricle—Endocardial and epicardial surfaces were created from LV contours (Rapidform; INUS Technology, Inc, Sunnyvale, CA). The space between the two surfaces was filled with 3648 8-node trilinear brick elements to generate a volumetric mesh that was 4 elements thick (Truegrid; XYZ Scientific Applications, Inc, Livermore, CA) (Figure 2B).

Myofiber angles at the epicardium and endocardium were assigned to be -60° and 60° with respect to the circumferential direction (counterclockwise positive when viewed in the base-to-apex direction), respectively. The myofiber angle was prescribed to vary linearly across the LV wall [18].

Three distinct material regions were assigned in the LV, namely, the infarcted region, the BZ region and the healthy remote region. The akinetic (i.e. no change in wall thickness in a cardiac cycle) infarct region was defined to be the region where the ventricular wall has thickness less than 6mm [8]. The BZ region with reduced contractility was defined to be the region adjacent to the infarct and was prescribed a width of 3cm [12]. The rest of the LV was defined to be the healthy remote region (Figure 2C).

2.3.2 Material law and parameters—Constitutive law describing passive filling of the LV was prescribed to the entire LV using the strain energy function

$$W = \frac{C}{2}\left(exp\left(b_f E_{ff}{}^2 + b_t(E_{ss}{}^2 + E_{nn}{}^2) + b_{fs}(E_{fs}{}^2 + E_{sf}{}^2 + E_{fn}{}^2 + E_{nf}{}^2)\right) - 1\right). \quad (1)$$

The strain energy function in Equation (1) is transversely isotropic with respect to the local fiber direction [7]. In this equation, C, b_f, b_{fs} and b_t are the diastolic myocardial material parameters and E_{ij} with subscripts $\{i, j\} \in \{f, s, n\}$ are the components of the Green strain tensor $\mathbf{E}$ where f, s and n denote the fiber, cross-fiber and transverse-fiber directions, respectively. The values of the material parameters in the exponent of Equation (1) were obtained from sheep with $b_f = 49.25$, $b_{fs} = 17.44$ and $b_t = 19.25$ in the entire LV [19]. Material parameter C at the infarct (C_I) was defined to be ten times stiffer than that in the remote (C_R) and in the BZ (C_{BZ}) i.e. $C_I = 10 C_R = 10 C_{BZ}$ [21]. The C – values were then scaled accordingly so that the LV EDV matched the measurement from CT images.

The assumption of near incompressibility of the LV requires the decoupling of strain energy function W into a dilational part U and a non-dilational part $\tilde{W}$. The dilational part U depends on the Jacobian J of the deformation gradient tensor and the non-dilational part $\tilde{W}$ depends on $\tilde{\mathbf{C}}$, which is the deviatoric decomposition of the right Cauchy-Green deformation tensor $\mathbf{C}$ (i.e. $\tilde{\mathbf{C}} = J^{2/3}\, \tilde{\mathbf{C}}$). The dilational part was prescribed the function $U = \frac{\kappa}{2}(J - 1)^2$ and the resultant second Piola-Kirchkoff (PK2) stress during diastole becomes

$$\boldsymbol{S} = \kappa\,(J - 1)\,J\mathbf{C}^{-1} + 2J^{-\frac{2}{3}} Dev\left(\frac{\partial \tilde{W}}{\partial \tilde{\mathbf{C}}}\right). \quad (2)$$

In Equation (2), bulk modulus κ was prescribed a value close to that of water (1040 kg/m^3) and Dev is the deviatoric projection operator defined as

$$Dev(\cdot) = (\cdot) - \frac{1}{3}([\cdot]:\mathbf{C})\mathbf{C}^{-1}. \quad (3)$$

Contraction during systole was modeled by adding an active stress component T_0 in the fiber direction f to the RHS of Equation (2) i.e. adding $T_0 \boldsymbol{f} \otimes \boldsymbol{f}$. The active stress T_0 that developed during systole is defined by a time-varying elastance model [6], where

$$T_0 = \frac{1}{2}T_{max}\frac{Ca_0^2}{Ca_0^2 + ECa_0^2}\left(1 - cos\left(\frac{0.25}{m\ell_R\,\sqrt{2E_{ff}+1}+b}+1\right)\pi\right). \quad (4)$$

In Equation (4), the active stress T_0 is a function of the fiber strain E_{ff}, the stress-free sarcomere length ℓ_R, the length-dependent calcium sensitivity ECa_0, the intracellular calcium concentration Ca_0 and the maximum isometric tension achieved at the longest sarcomere length T_{max}. The length-dependent calcium sensitivity was defined by

$$ECa_0 = \frac{Ca_{0,max}}{\sqrt{exp(B\ell_R\,\sqrt{2E_{ff}+1} - \ell_0) - 1}}, \quad (5)$$

where ℓ_0 is the sarcomere length at which no active tension develops and $Ca_{0,\max}$ is the maximum peak intracellular concentration. Based on large animal studies, the material constants in the time-varying elastance model were prescribed values $Ca_0 = 4.35\mu mol/l$,

$Ca_{0,max} = 4.35\mu mol/l$, $B = 4.75\mu m^{-1}$, $\ell_0 = 1.58\mu m$, $m = 1.0489s\ \mu m^{-1}$, $b = -1.429s$ and $\ell_R = 1.85\mu m$ [24].

To reflect the regional contractile state of the infarcted LV, T_{max} of the infarct (T_{max_I}) and the remote region (T_{max_R}) were adjusted so that: (a) the predicted LV ESV matched the measurements from CT images and (b) the average difference of the infarct thickness at ED and ES was zero. The latter criterion reflects akinesis of the infarct [3]. Across the borderzone, T_{max} was prescribed to vary linearly (from T_{max_I} to T_{max_R}) with distance measured from infarct [12].

These active and passive constitutive laws were implemented using a user-defined material subroutine in LS-DYNA.

2.3.3 Boundary conditions—The LV base was constrained from moving in the longitudinal direction (i.e. in the apex-base direction) and the epicardial-basal edge was fixed in space (Figure 2D). Because the velocity of the blood is quite small at ED and ES, which coincide with the end of filling and end of ejection in a cardiac cycle respectively, the pressure gradient within the LV is quite small [20]. Consequently, we prescribed a uniform pressure distribution at the LV endocardial wall based on the measured pressure data presented in the "Clinical data" section (Figure 2D). Specifically, the LV EDP was prescribed to be 20 mm Hg in both PRE-OP and VIRTUAL-Parachute cases, and 12 mm Hg in the POST-OP case. The LV end-systolic pressure (ESP) was prescribed to be 120 mm Hg in all cases.

2.3.4 Parachute® model—The Parachute® consists of an expanded polytetrafluoroethylene (ePTFE) membrane bonded to an expanded Nitinol frame. The Nitinol frame consists of 16 struts and is attached to a radioplaque foot. The approximate diameter of the Parachute® is 85mm. An FE model of the Parachute® was created (Figure 3A). Specifically, the Nitinol frame, ePTFE membrane and foot were modeled using 496 beam elements, 1152 shell elements and 1110 solid elements, respectively. Isotropic and linear elastic material law was assigned to these 3 components and the material parameters are tabulated in Table 1.

2.3.5 Virtual implantation of the Parachute® device—In the actual implantation process, the Parachute® is first collapsed and then delivered percutaneously from the femoral artery by standard catheterization technique. Once in position, the Parachute® is expanded and the anchor tip of each strut in the device engages and hooks on to the LV endocardial wall. As a result, the struts are not "stress-free" after implantation in the LV.

To account for residual stress in the struts and LV after implantation, the Parachute® implantation process was also simulated. First, the Parachute® was collapsed by applying a constant follower force at the end of each strut in order for it to not come into contact with the LV (Figure 3B).

Next, the follower force was removed and a contact constraint between the LV endocardium and the Parachute® was activated. Consequently, the Parachute® Nitinol frame expanded

and came into contact with the LV endocardium. To simulate the anchor tip of each strut hooking onto the LV endocardial wall after implantation, the nodal tip of each strut was tied to the endocardial wall upon contact (Figure 3C). The virtual implantation process is also shown in Online Resource 2.

The deployed position of the Parachute® in the LV was adjusted based on CT images taken from the same patient 6 months after implantation. In its deployed position, the Parachute® partitioned the LV into two chambers, namely, a lower static chamber containing mostly the infarct and an upper functional chamber containing mostly the remote healthy tissue. Two cardiac phases, namely, ED and ES, were simulated from this configuration.

Because leaks between the upper and lower chambers were found to be small based on Doppler echocardiography, EDP and ESP in the lower chamber were adjusted so that the lower chamber had a constant volume of about 36.2 ml (based on CT measurements). The ESP in the upper chamber was kept at the baseline value of 120 mmHg and the EDP was adjusted to match clinical data as described in the section "Boundary conditions".

2.4 Statistical and sensitivity analysis

Stress and strain were averaged over all elements in each of the two partitioned regions (upper and lower chambers) within the LV and were presented as average ± standard deviation. A single FE model based on a patient was used. The results obtained are not stochastic and statistical tests are therefore not appropriate. P values are therefore not reported. To account for changes of the myofiber stress due to a variation of model parameters, we performed a sensitivity analysis in which we analyzed the effects on myofiber stress due to changes in the extent of infarct dysfunction, the degree of infarct anisotropy, the myofiber angles and the borderzone width (see Online Resource 3).

3. Results

3.1 Clinical data

Parachute® implantation for this patient was performed at the Texas Heart Institute as part of the multi-center, phase 1 'Parachute United States Feasibility Trial' clinical trial. The study protocol was approved by the Texas Heart Institute Institutional Review Board (IRB). Subsequent analysis of radiographic images obtained from this patient was approved by the Committee on Human Research of the University of California, San Francisco.

The patient was a single 52-year-old male whose status was 9-years post large, antero-apical MI. The procedure was uneventful and there were no complications at one-year follow up. Before Parachute® implantation, his NYHA class was 3 and it improved to 1 at one-year follow up.

Computed tomography images were obtained before and 6 months after Parachute® implantation. The PRE-OP and 6-month POST-OP volumes are given in Table 2. Left ventricular volume at ED and ES were reduced after 6 months by 4.4% and 5.7%, respectively. On the other hand, comparison between the volume of the functioning chamber at 6-months POST-OP (upper chamber) and that at PRE-OP (entire LV chamber), showed

reductions in EDV and ESV by 20.7% and 25.3%, respectively. The PRE-OP ejection fraction was 27.7% and upper chamber ejection fraction at 6-months POST-OP was 31.9%. Stroke volume was essentially unchanged at 6-months POST-OP.

In ten other patients who underwent the Parachute® procedure as part of the 'Parachute United States Feasibility Trial' [13, 15], the LV EDP was measured to be 18.2 ± 8.2 mmHg and 12.9 ± 4.5 mmHg (p<0.05) at PRE-OP and 6-months POST-OP, respectively.

3.2 PRE-OP Model

Regional LV material parameters assigned to the PRE-OP model are shown in Table 3 and the resultant regional variation of contractility $T_{\max}$ is shown graphically in Figure 2C. The infarct contractility ($T_{\max\_I} = 117$ kPa) was found to be 60% that of the remote contractility ($T_{\max\_R} = 195$kPa) in order for the average difference between the infarct thickness at ED and ES to be zero. In the 3cm BZ, the resultant contractility therefore varied linearly from 117 kPa to 195 kPa with distance measured from the infarct.

The FE model of the LV (Figure 2C) closely resembles that in the PRE-OP CT images (Figure 2A) showing the thin antero-apical infarct region. As seen in Table 2, the PRE-OP LV EDV and ESV were within 7.7% and 10.9% of the PRE-OP CT data, respectively.

3.3 Acute mechanical effect of Parachute® (VIRTUAL-Parachute)

The VIRTUAL-Parachute model shown in Figure 3C qualitatively resembles the CT images in Figure 1 showing the LV at 6 months after implantation. Apparent in these 2 figures, the apical infarct and part of the BZ were covered by the Parachute® (see Online Resource 2). The total contact force exerted by the Parachute® on the LV after implantation is 2.3N

The effects of VIRTUAL-Parachute on LV volumes and pressures are shown in Table 2. First, to maintain a lower chamber volume of about 36.2 ml throughout the cardiac cycle, the lower chamber pressure was predicted to be less than that in the upper chamber, which was held equal to that in the PRE-OP model. At ED and ES, the lower chamber pressures were predicted to be 72.5% and 4.8% lower than that in the upper chamber, respectively.

Also, the VIRTUAL-Parachute model predicted a reduction in the LV volume at ED (4.3%) and ES (0.2%). As a result, stroke volume was predicted to decrease by 13.6%.

3.4 Chronic effect of Parachute® (6 month POST-OP)

To better match the LV volume measurements from the 6-month POST-OP CT images (in particular, the measured stroke volume) and to account for the decrease in LV EDP 6 months after Parachute® implantation, the LV material parameters were adjusted. These parameters are given in Table 3. We found that a 63.6% reduction in LV passive stiffness can better predict the 6-month LV volume measurements. Specifically, the predicted EDV and ESV were within 3% and 3.1% of the measurements, respectively. Also with that adjustment, the predicted stroke volume was within 2.8% of the measurement.

3.5 Myofiber stress

Residual myofiber stress in the LV immediately after implantation of the Parachute® was 0.06 kPa. The effects of the Parachute® on LV regional myofiber stress at ED and ES are tabulated in Table 4 and shown graphically in Figure 4. Because the LV wall at the antero-apical infarct was substantially thinner than that in the remote region, myofiber stress was predicted to be elevated in that region in the PRE-OP model. Specifically, myofiber stress in the antero-apical region (lower chamber) was about twice as large as that in the remote region (upper chamber) at ED and ES.

However, as a result of the reduction in the lower-chamber-EDP predicted in the VIRTUAL-Parachute model, the average ED myofiber stress in the lower chamber was reduced by 61.2 % (from 11.6 ± 8.2 kPa to 4.5 ± 3.8 kPa). By contrast, the average ED myofiber stress in the upper chamber was essentially unchanged in the VIRTUAL-Parachute model. Also, end-systolic myofiber stress in both chambers was predicted to be unaffected by Parachute® implantation.

Compared to the VIRTUAL-Parachute model, the POST-OP model predicted a greater decrease in ED myofiber stress in the lower chamber (78.4%). In addition, the POST-OP model also predicted a 27.1% decrease in ED myofiber stress (from 5.9 ± 4.5 kPa to 4.3 ± 3.9 kPa) in the upper chamber. The combined average myofiber stress in both chambers was 59.5% lower than that in the PRE-OP model. End-systolic myofiber stress in both chambers, however, was essentially unchanged in the POST-OP model.

Results from the sensitivity analysis (Online Resource 3) show that the greatest absolute changes in myofiber stress due to a change in the myofiber angles, the degree of infarct anisotropy, the extent of infarct dysfunction and the borderzone width were 9.6%, 16.8%, 13.7% and 1.3%, respectively. Thus, the changes in myofiber stress caused by a variation of these parameters were relatively small when compared to the predicted decrease in ED myofiber stress (59.5%) between the POST-OP and PRE-OP model.

4. Discussion

The principal finding of this study is that implantation of the Parachute® in the LV with antero-apical infarct substantially reduced myofiber stress at ED. The ED myofiber stress was predicted to decrease only in the partitioned lower chamber when the effects immediately after Parachute® implantation were considered alone (VIRTUAL-Parachute case). However, myofiber stress at ED was reduced in both upper and lower chambers after the LV material parameters were adjusted to better match the 6-month POST-OP CT and LV EDP data.

4.1 Parachute® model

We have presented the first patient-specific mathematical model of a human LV implanted with the Parachute®. The model is realistic because in addition to simulating a beating LV implanted with this device, the entire Parachute® implantation process was also simulated to account for possible influence of the residual stress on the LV function and regional myofiber stress. We found that residual stress in the LV associated with Parachute®

implantation is small — about an order of magnitude smaller than the ED myofiber stress. This result is also consistent with our results, which show that the total contact force of 2.3N exerted by the Parachute® on the LV wall is small compared to the total pressure force (product of pressure and endocardial surface area) exerted on the LV wall. In the VIRTUAL-Parachute case, the total pressure force was predicted to be about 30N and 200N at ED and ES, respectively.

4.2 Effects on myofiber stress

Results from this single patient study suggest that the therapeutic effects associated with Parachute® implantation observed in humans [2, 15] and sheep [14] may possibly have come from a reduction in pressure exerted on the partitioned lower chamber wall of the LV at ED. The lowered pressure acting on the infarct reduces myofiber stress in the LV. In the POST-OP case, ED myofiber stress across the entire LV was reduced by 59.5% on average and its distribution became more homogeneous (Figure 4). Since elevated myofiber stress is widely believed to be responsible for adverse cardiac remodeling [5], the reported therapeutic effects are probably an outcome of the local reduction in the infarct myofiber stress as predicted by our simulation.

4.3 Acute and chronic effects on LV pump function

The VIRTUAL-Parachute simulation predicted that both EDV and ESV would be reduced immediately after Parachute® implantation. Because the reduction in EDV was larger than the reduction in ESV, stroke volume was also predicted to have reduced (-13.6%) immediately after implantation. A reduction in stroke volume is also found in simulations of other treatments such as Surgical Ventricular Restoration [11]. However, based on the CT data, stroke volume was largely restored at 6 months (-1.0%). It is interesting that in order to match the 6-month CT data, the diastolic stiffness parameter C had to be significantly reduced in the POST-OP model. Further work is needed in this area. However, it is possible that the change in diastolic stiffness is a result of favorable LV remodeling.

4.4 Left ventricle with infarct

We modeled the LV BZ as a region having contractility that varies linearly with distance from the infarct because in a previous sheep study, such a BZ model had predicted strain that better matched the *in vivo* strain measurements [12]. With such a BZ model, contractility of the entire LV depends on 2 parameters, namely, contractility in the akinetic infarct ($T_{\max\_I}$) and the remote region ($T_{\max\_R}$). We found that the predicted akinetic infarct contractility was 60% of that in the remote region. This value is close to that found in sheep, where in a study by Dang et al. [3], the infarct contractility required to produce akinesis was 50% of that in the remote region when the infarct passive stiffness C_I is 10 times that of the remote region C_R i.e. $C_I = 10C_R$. This passive stiffness ratio (which was used in our models) is based on previous sheep studies [21].

4.5 Limitations

Our model has 3 main limitations. First, given that the sole purpose was to evaluate the effects of the Parachute® on the LV, we have simplified the analysis by modeling the

Nitinol strut using beam elements. Second, we did not acquire *in vivo* myocardial regional strain data because the patient had contraindications to magnetic resonance imaging (MRI). Consequently, the model could not be validated against regional myocardial MRI-based strain measurements. To corroborate the model's prediction, new methods to quantify regional myocardial contraction in CT images [16, 17] could be used in future studies. Last, we do not have pressure measurements in the lower chamber (which are difficult to obtain) to corroborate our prediction of the lower chamber pressure. Modeling blood flow in the LV after Parachute® implantation can help to provide a more direct quantification of the pressure difference between the upper and lower chamber, as well as the pressure differential within the partitioned chambers.

4.6 Conclusion and future directions

In conclusion, we have created the first realistic FE model of the Parachute® implanted in a human LV, including the implantation process. We have quantified the effects of this treatment on both LV function and regional myofiber stress. Results from this single-patient study suggest that the device reduces ED myofiber stress in the LV, particularly in the partitioned lower chamber. These results are preliminary and studies involving more patients are necessary to fully understand the effects of the Parachute®. Nonetheless, the methodology described here opens the way for future FE studies of this novel device.

Supplementary Material

Refer to Web version on PubMed Central for supplementary material.

Acknowledgments

References

1. Anand IS, Liu D, Chugh SS, Prahash AJ, Gupta S, John R, Popescu F, Chandrashekhar Y. Isolated myocyte contractile function is normal in postinfarct remodeled rat heart with systolic dysfunction. Circulation. 1997; 96:3974–84. [PubMed: 9403622]

2. Bozdag-Turan I, Bermaoui B, Turan RG, Paranskaya L, G DA, Kische S, Hauenstein K, Nienaber CA, Ince H. Left ventricular partitioning device in a patient with chronic heart failure: Short-term clinical follow-up. Int J Cardiol. 2012; 163:e1–e3. [PubMed: 22824252]

3. Dang AB, Guccione JM, Mishell JM, Zhang P, Wallace AW, Gorman RC, Gorman JH 3rd, Ratcliffe MB. Akinetic myocardial infarcts must contain contracting myocytes: finite-element model study. Am J Physiol Heart Circ Physiol. 2005; 288:H1844–50. [PubMed: 15604126]

4. Dang AB, Guccione JM, Zhang P, Wallace AW, Gorman RC, Gorman JH 3rd, Ratcliffe MB. Effect of ventricular size and patch stiffness in surgical anterior ventricular restoration: a finite element model study. Ann Thorac Surg. 2005; 79:185–93. [PubMed: 15620941]

5. Grossman W, Jones D, McLaurin LP. Wall stress and patterns of hypertrophy in the human left ventricle. J Clin Invest. 1975; 56:56–64. [PubMed: 124746]

6. Guccione JM, Waldman LK, McCulloch AD. Mechanics of active contraction in cardiac muscle: Part II--Cylindrical models of the systolic left ventricle. J Biomech Eng. 1993; 115:82–90. [PubMed: 8445902]

7. Guccione JM, Costa KD, McCulloch AD. Finite element stress analysis of left ventricular mechanics in the beating dog heart. J Biomech. 1995; 28:1167–77. [PubMed: 8550635]

8. Gutberlet M, Frohlich M, Mehl S, Amthauer H, Hausmann H, Meyer R, Siniawski H, Ruf J, Plotkin M, Denecke T, Schnackenburg B, Hetzer R, Felix R. Myocardial viability assessment in patients with highly impaired left ventricular function: comparison of delayed enhancement, dobutamine stress MRI, end-diastolic wall thickness, and TI201-SPECT with functional recovery after revascularization. Eur Radiol. 2005; 15:872–80. [PubMed: 15754164]

9. Huisman RM, Elzinga G, Westerhof N, Sipkema P. Measurement of left ventricular wall stress. Cardiovascular Research. 1980; 14:142–53. [PubMed: 7397716]

10. Jackson BM, Gorman JH, Moainie SL, Guy TS, Narula N, Narula J, John-Sutton MG, Edmunds LH Jr, Gorman RC. Extension of borderzone myocardium in postinfarction dilated cardiomyopathy. J Am Coll Cardiol. 2002; 40:1160–7. discussion 1168-71. [PubMed: 12354444]

11. Jones RH, Velazquez EJ, Michler RE, Sopko G, Oh JK, O'Connor CM, Hill JA, Menicanti L, Sadowski Z, Desvigne-Nickens P, Rouleau J-L, Lee KL. STICH Hypothesis 2 Investigators. Coronary Bypass Surgery with or without Surgical Ventricular Reconstruction. N Engl J Med. 2009; 360:1705–17. [PubMed: 19329820]

12. Lee LC, Wenk JF, Klepach D, Zhang Z, Saloner D, Wallace AW, Ge L, Ratcliffe MB, Guccione JM. A novel method for quantifying in-vivo regional left ventricular myocardial contractility in the border zone of a myocardial infarction. J Biomech Eng. 2011; 133:094506. [PubMed: 22010752]

13. Mazzaferri EL Jr, Gradinac S, Sagic D, Otasevic P, Hasan AK, Goff TL, Sievert H, Wunderlich N, Nikolic SD, Abraham WT. Percutaneous left ventricular partitioning in patients with chronic heart failure and a prior anterior myocardial infarction: Results of the PercutAneous Ventricular RestorAtion in Chronic Heart failUre PaTiEnts Trial. Am Heart J. 2012; 163:812–820 e1. [PubMed: 22607859]

14. Nikolic SD, Khairkhahan A, Ryu M, Champsaur G, Breznock E, Dae M. Percutaneous implantation of an intraventricular device for the treatment of heart failure: experimental results and proof of concept. J Card Fail. 2009; 15:790–7. [PubMed: 19879466]

15. Sagic D, Otasevic P, Sievert H, Elsasser A, Mitrovic V, Gradinac S. Percutaneous implantation of the left ventricular partitioning device for chronic heart failure: a pilot study with 1-year follow-up. Eur J Heart Fail. 2010; 12:600–6. [PubMed: 20400453]

16. Pourmorteza A, Schuleri KH, Herzka DA, Lardo AC, McVeigh ER. Regional cardiac function assessment in 4D CT: comparison between SQUEEZ and ejection fraction. Conf Proc IEEE Eng Med Biol Soc. 2012; 2012:4966–9. [PubMed: 23367042]

17. Pourmorteza A, Schuleri KH, Herzka DA, Lardo AC, McVeigh ER. A new method for cardiac computed tomography regional function assessment: stretch quantifier for endocardial engraved zones (SQUEEZ). Circ Cardiovasc Imaging. 2012; 5:243–50. [PubMed: 22342945]

18. Streeter DD, Spotnitz HM, Patel DP, Ross J Jr, Sonnenblick EH. Fiber orientation in the canine left ventricle during diastole and systole. Circ Res. 1969; 24:339–47. [PubMed: 5766515]

19. Sun K, Stander N, Jhun CS, Zhang Z, Suzuki T, Wang GY, Saeed M, Wallace AW, Tseng EE, Baker AJ, Saloner D, Einstein DR, Ratcliffe MB, Guccione JM. A computationally efficient formal optimization of regional myocardial contractility in a sheep with left ventricular aneurysm. J Biomech Eng. 2009; 131:111001. [PubMed: 20016753]

20. Thompson RB, McVeigh ER. Fast measurement of intracardiac pressure differences with 2D breadth-hold phase-contrast MRI. Magn Reson Med. 2003; 49:1056–66. [PubMed: 12768584]

21. Walker JC, Ratcliffe MB, Zhang P, Wallace AW, Fata B, Hsu EW, Saloner D, Guccione JM. MRI-based finite-element analysis of left ventricular aneurysm. Am J Physiol Heart Circ Physiol. 2005; 289:H692–700. [PubMed: 15778283]

22. Walker JC, Ratcliffe MB, Zhang P, Wallace AW, Hsu EW, Saloner DA, Guccione JM. Magnetic resonance imaging-based finite element stress analysis after linear repair of left ventricular aneurysm. J Thorac Cardiovasc Surg. 2008; 135:1094–102. 1102 e1–2. [PubMed: 18455590]

23. Wenk JF, Sun K, Zhang Z, Soleimani M, Ge L, Saloner D, Wallace AW, Ratcliffe MB, Guccione JM. Regional left ventricular myocardial contractility and stress in a finite element model of posterobasal myocardial infarction. J Biomech Eng. 2011; 133:044501. [PubMed: 21428685]

24. Wenk JF, Klepach D, Lee LC, Zhang Z, Ge L, Tseng EE, Martin A, Kozerke S, Gorman JH 3rd, Gorman RC, Guccione JM. First evidence of depressed contractility in the border zone of a human myocardial infarction. Ann Thorac Surg. 2012; 93:1188–93. [PubMed: 22326127]
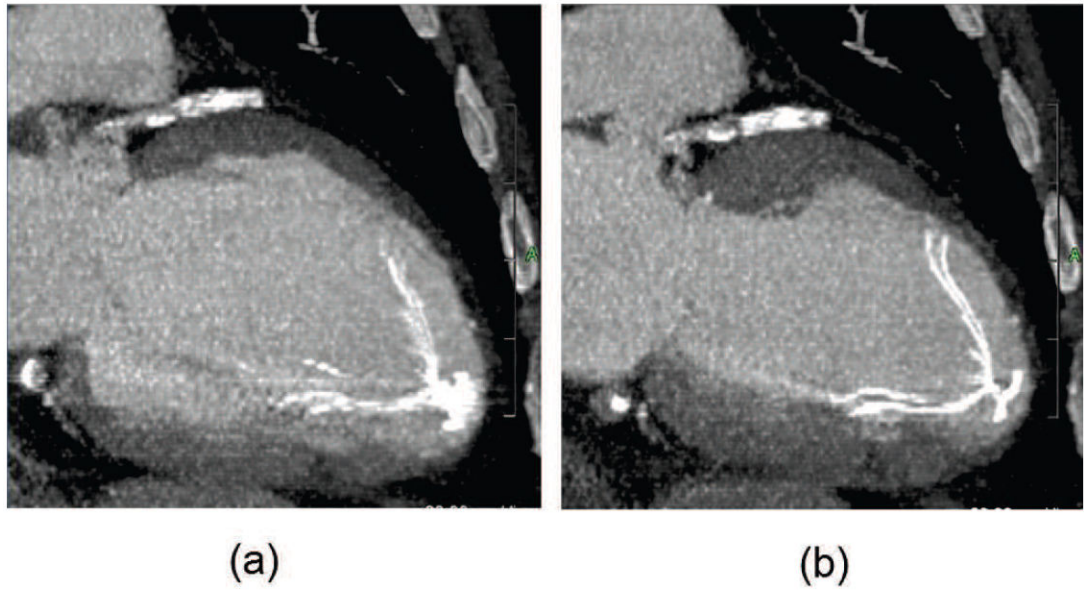
Fig. 1.
CT images of the left ventricle 6 months after Parachute® implantation: (a) end-diastole and (b) end-systole.
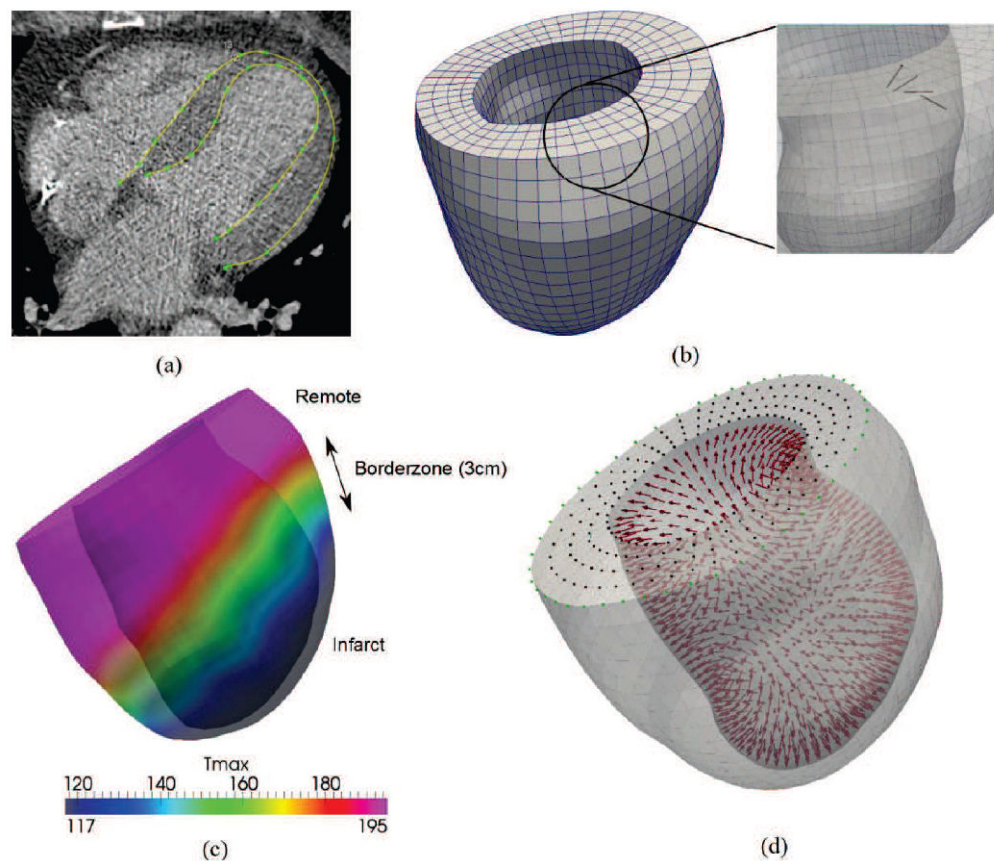
Fig. 2.
Construction of the patient-specific finite element LV model: (a) Digitization of the endocardial and epicardial surfaces, (b) fiber orientation in the finite element LV model, (c) regional contractility in the LV with infarct and (d) boundary conditions prescribed on the LV – green dots, black dots and red arrows indicate epicardial-basal edge displacement constraints, basal displacement constraints and prescribed pressure on endocardial wall, respectively.
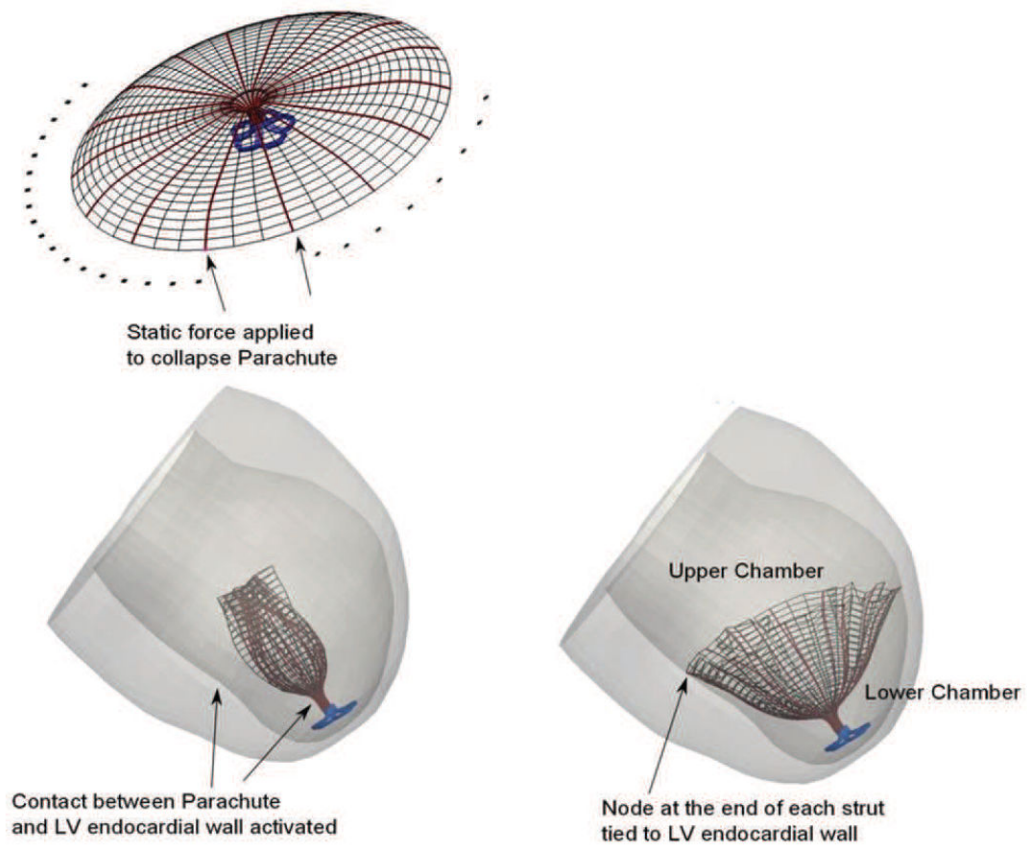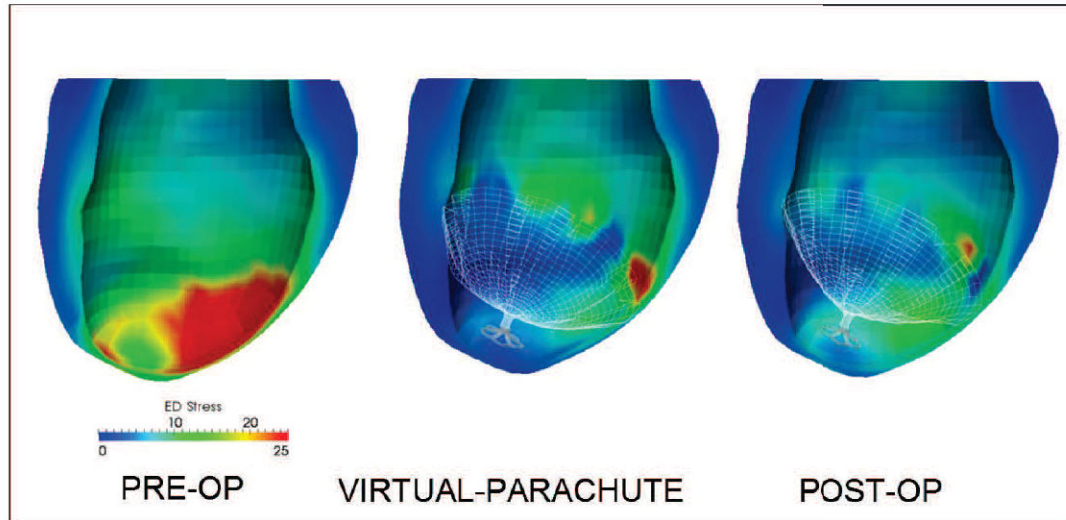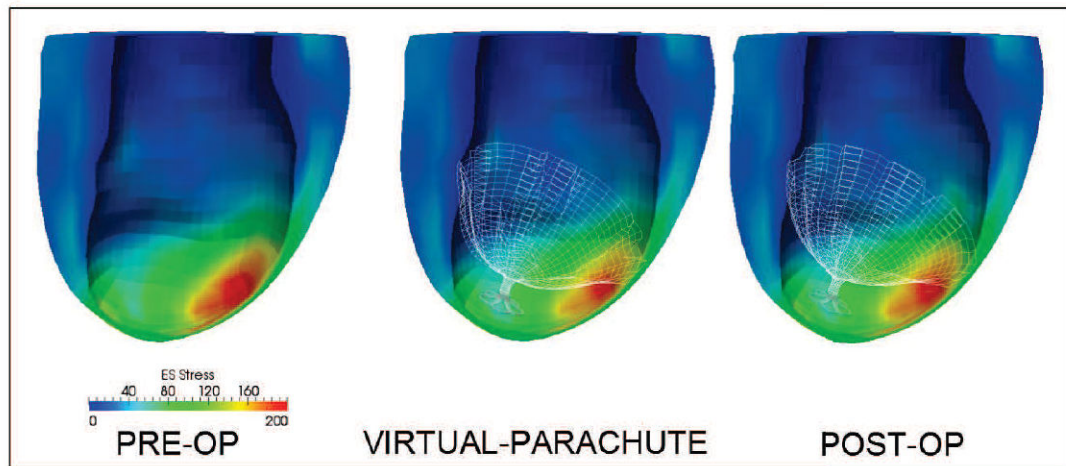
Fig. 3.
Virtual implantation of the Parachute® into the left ventricle: (a) finite element model of the Parachute® in which the struts of the Nitinol frame are shown in red, (b) the collapsed Parachute®, (c) the implanted Parachute®. Refer to text for explanation.

Fig. 4.
Effects of Parachute® on the left ventricular regional myofiber stress: (a) end-diastole and (b) end-systole. Color scale units are kPa.

Table 1

Material parameters of components in the Parachute®. Unit of the elastic modulus is MPa.

Component	Elastic Modulus	Poisson Ratio
Nitinol Frame	33.73×10^3	0.33
Foot	20	0.45
ePTFE Membrane	400	0.33

Table 2

Left ventricular volumes and pressures before and after Parachute® implantation.

	Lower ED Volume	Upper ED Volume	Total ED Volume	Lower ES Volume	Upper ES Volume	Total ES Volume	Stroke Volume	Lower ED Pressure	Lower ES Pressure	Upper ED Pressure	Upper ES Pressure
CT Scan: PRE-OP	-	-	222.8	-	-	161.0	61.8	-	-	18.2*	Not measured
FE Model: PRE-OP	-	-	205.7	-	-	143.4	62.3	-	-	20	120
CT Scan: 6 months POST-OP	36.2	176.7	212.9	31.8	120.3	151.8	61.2	Not measured	Not measured	12.9*	Not measured
FE Model: VIRTUAL-Parachute	36.7	160.2	196.9	35.7	107.4	143.1	53.8	5.5	114.3	20	120
FE Model: 6 months POST-OP	39.2	167.4	206.6	38.3	108.8	147.1	59.5	2.5	114.3	12	120

(*) denotes the average value measured in 10 other patients as described in the "Clinical data" section. (-) indicates data that are irrelevant to the unpartitioned PRE-OP FE model and CT scan. Pressures in the PRE-OP case correspond to the entire LV chamber, which is not partitioned.

ED = end-diastole, ES = end-systole, Lower = lower chamber, Upper = upper chamber. Volume units are [ml] and pressure units are [mm Hg].

Table 3

Left ventricular regional material parameters. Unit is kPa.

	Infarct passive stiffness (C_I)	Remote passive stiffness (C_R)	Infarct contractility (T_{max_I})	Remote contractility (T_{max_R})
FE Model: PRE-OP	2.75	0.275	117	195
FE Model: VIRTUAL-Parachute	2.75	0.275	117	195
FE Model: 6 months POST-OP	1.0	0.10	117	195

NIH-PA Author Manuscript

NIH-PA Author Manuscript

NIH-PA Author Manuscript

Table 4

Effects of Parachute® on left ventricular myofiber stress.

	Lower Chamber Stress at ED	Upper Chamber Stress at ED	Left Ventricular Stress at ED	Lower Chamber Stress at ES	Upper Chamber Stress at ES	Left Ventricular Stress at ES
FE Model: PRE-OP	11.6 ± 8.2	5.9 ± 4.5	8.4 ± 7.1	66.6 ± 48.6	31.6 ± 23.8	47.2 ± 41.3
FE Model: VIRTUAL- Parachute	4.5 ± 3.8	5.8 ± 4.7	5.1 ± 4.1	64.2 ± 45.7	32.0 ± 23.7	46.2 ± 38.9
FE Model: 6 months POST-OP	2.5 ± 3.0	4.3 ± 3.9	3.4 ± 3.4	67.7 ± 49.3	32.2 ± 25.1	47.9 ± 42.1

ED = end-diastole, ES = end-systole. Unit is kPa.